Optics and Laser Technology xxx (xxxx) xxx-xxx

Contents lists available at ScienceDirect

Optics and Laser Technology

journal homepage: http://ees.elsevier.com

Influence of Al doping on random lasing in ZnO nanorods

N. Fadzliana [a], S.A.M. Samsuri [a], S.Y. Chan [b], H.C. Hsu [b], W. Maryam [a,*]

[a] School of Physics, Universiti Sains Malaysia, 11800 Penang, Malaysia
[b] Department of Photonics, National Cheng Kung University, Tainan 70101, Taiwan

A B S T R A C T

Random lasing was demonstrated from aluminum doped ZnO nanorods fabricated on ITO coated glass substrates using simple chemical deposition technique. Different Aluminum (Al) doping parameters were explored in an attempt to realize low threshold ZnO random lasers. Results confirm threshold was strongly dependent on doping concentration and suggestive of resonant coupling with Al in lowering the threshold by 2 orders of magnitude when compared to undoped ZnO nanorods. Lowest threshold was obtained from ZnO nanorods doped with 10 mM of aluminum, suggesting best doping concentration for ZnO random lasers formed by nanorod array. Results further indicate possibility of controlling random lasing properties by adjusting the doping concentration.

1. Introduction

Lasing from nanoscale devices, specifically random lasers have the added advantage of lasing without the need of a conventional cavity made of mirrors whereby the "cavity" is made of the scattering random media [1]. In coherent random lasers, multiple modes of lasing appears above the broad spontaneous emission peak [2–6]. Various method have been proposed to reduce the threshold in these random lasers such as by laser-induced hydrothermal synthesis [7], introducing point defects using polymer particles [8], utilizing defect pits [9], tapering nanowires [10], reducing crystallite size [11], using colloidal nanoparticles [12], gold nanoparticles [13] etc. Here we wish to demonstrate the role of doping in reducing the threshold of ZnO random lasers.

The doping procedure can be utilized to optimize materials compositions in order to improve laser emission parameters [14]. For instance, rare earth have been used as dopants in chalcogenide glass to achieve lasing [15]. On the other hand, specific doping techniques have been developed to improve nanolasers [16] and to obtain high optical gain for CMOS integrated laser emissions [17]. In some specific cases, doping has also been shown to improve gain and modulation bandwidth, for example in InGaAsP lasers [18]. By providing the right doping, a material may also act as the core-fiber material of an optical amplifier [19]. In random lasers, polymer can be doped with dyes to reduce the threshold in polymeric random lasers [20] and doping ZnO with polystyrene particles provided means of tuning multimode random lasers into single mode random lasers [21]. However, the size of the doped particles in the latter case was close to 1 µm in diameter and provided additional voids between the ZnO spheres. In this work, the doping act as point defects within the ZnO structure.

Our present work is designed to show how doping ZnO nanorods with aluminum would reduce the threshold of ZnO random lasers. The nanorods were prepared on pretreated ITO coated glass substrates by improved chemical bath deposition process for better uniformity of the nanorods [22,23]. The effect on nanorod morphology and crystallinity due to the doping that may affect lasing is discussed. Defect emissions were observed from photoluminescence measurements whereas random lasing measurements revealed the influence of doping concentration on lasing threshold. Threshold was at least 8 times smaller in doped samples and lowest threshold was achieved when 10 mM alumina concentration was used. Our results also suggest that doping with alumina may be used as mode control in random lasers.

2. Experimental methods

In our CBD technique, all chemicals were used without further purification and the aqueous solution was prepared using deionized water. The ITO glass substrate was pre-coated with 50 nm of ZnO thin film using radio frequency magnetron sputtering. The CBD solution was prepared by mixing 0.08 M of zinc nitrate ($Zn(NO_3)_2{\cdot}6H_2O$), 0.08 M hexamethylenetetramine (HMT) and 5, 10, 30 and 50 mM aluminium nitrate nonahydrate ($Al(NO_3)_3{\cdot}9H_2O$,) respectively as dopants. The pre-coated substrate was then placed vertically inside the beaker containing the solution and covered with aluminum foil. The solution was then heated in a binder oven for 50 min at a fixed

* Corresponding author.
E-mail address: wanmaryam@usm.my (W. Maryam)

https://doi.org/10.1016/j.optlastec.2019.106004
Received 21 May 2019; Received in revised form 29 November 2019; Accepted 1 December 2019
Available online xxx
0030-3992/© 2019.

temperature of 96 °C. The samples were then annealed at 300 °C in ambient air for 60 min. The undoped sample was prepared by the same method but without the dopant mixture.

The morphology of these nanorods were investigated by field emission scanning electron microscope (FESEM; Nova NanoSEM 450, FEI, Japan) integrated with energy dispersive X-ray (EDX) spectroscopy for determining elemental compositions of the samples. Photoluminescence from the sample was excited by CW HeCd laser source operating at 325nm whilst random lasing measurements were performed using a microPL system with an Nd:YAG pulsed laser source operating at 355 nm, 1 KHz rep rate and 350 ps pulse width. The sample holder was fixed onto a three axis translational stage to focus the laser light onto the sample which was observed from a camera mounted at an angle from the sample holder. The emitted radiation was collected into an optical fiber bundle connected to a spectrograph equipped with a liquid-N_2 CCD array detector. All measurements were performed at room temperature. The beam spot size was set to 100 μm in diameter.

3. Results and discussion

The morphology of these nanorods are shown in Fig. 1. Cross section images for measuring the average height is provided in the inset. The average density on the other hand was examined using Image J software and revealed, in general, a decreasing trend with increasing dopant concentration, from 153 nanorods/μm^2 to just 53 nanorods/μm^2 at 50 mM doping concentration. A decrease in growth rate when more Al dopants are introduced may be due to the presence of $Al(OH)_4^-$ impeding the growth along the c-axis as well as decelerating of growth by the pronounced precipitation of the solution [24]. This effect is obvious at high doping concentrations (Fig. 1(e)). Values are plotted together with the average nanorod height in Fig. 1(f). Based on the FESEM images, voids become more apparent with increasing alumina concentration, hence reducing the population density of the nanorods.

Photoluminescence from the sample is shown in Fig. 2(a). The UV emission at about 400 nm is the near band edge (NBE) emission of ZnO whilst the visible (green) emission is related to defects, mainly by oxygen vacancy and interstitial zinc as donor levels and

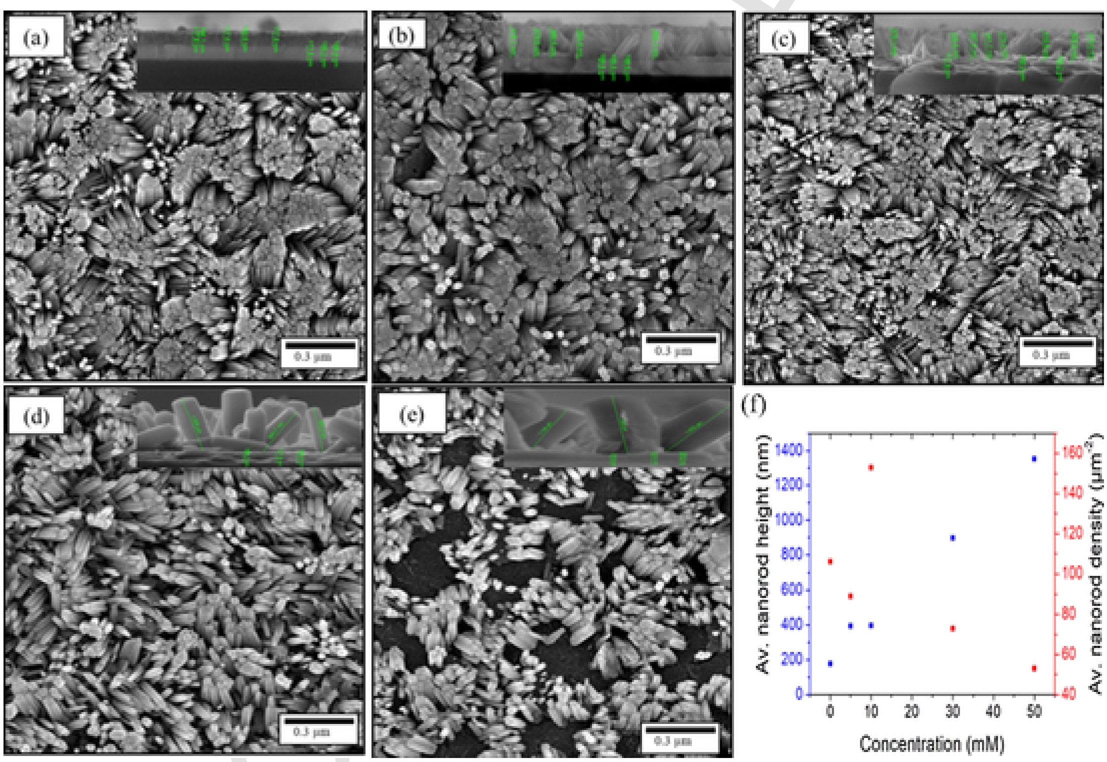

Fig. 1. (a–e): FESEM images of ZnO nanorods doped with 0, 5, 10, 30 and 50 mM of Aluminum concentration respectively. (f) Graph of average nanorod height and density with increasing aluminum concentration.

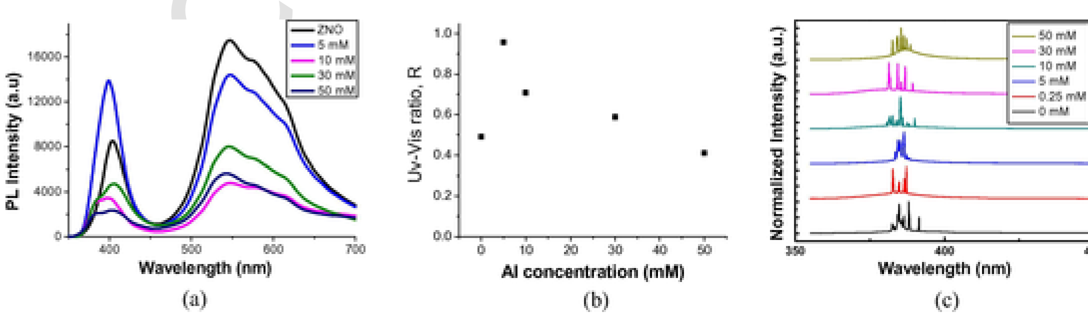

Fig. 2. (a) CW photoluminescence from ZnO nanorods showing band gap emission and defects related emission and (b) UV–Vis ratio, R, of the emission peaks for all samples. (c) Random lasing spectra at high pumping energy (2 mW) in all samples.

vacancy zinc as acceptor levels [25,26]. Upon evaluating the Uv–Vis ratio, R, as plotted in Fig. 2 (b), increasing the aluminum concentration during growth decreases the green emission as R increased from 0.49 for undoped samples to 0.97 for samples grown with 5 mM of aluminum concentration. This would occur when the doping process creates new donor sites that prevents donor bound excitons participating in the energy transfer to the green emitting sites [27]. However, increasing the aluminum concentration further has increased the green emission with respect to the NBE emission. This has been shown to occur in Al:ZnO when zinc vacancies are created during the doping process as well as oxygen vacancies created by the substitution of zinc atoms with Al leading to enhancement of the green emission [28,29].

Table 1 shows EDX results from all samples to determine atomic percentage of elements in the sample. In summary, the atomic percentage of Zn decrease and atomic percentage of O and Al increase with increasing aluminum concentration. This implies substitution of Zn sites by Al atoms and the doping of Al atoms in the interstitial sites owing to their smaller size than Zn atoms.

Table 1
EDX results showing atomic percentage of elements in each sample.

Aluminum Concentration (mM)	Atomic (%)		
	O	Al	Zn
0	46.53	0	53.47
5	50.78	0.52	48.70
10	55.47	0.67	43.86
30	54.74	0.99	44.27
50	60.12	2.39	37.49

Random lasing measurements were performed and lasing was observed in all samples but with different threshold values. Fig. 3 shows the results obtained from pure ZnO nanorods and aluminium doped ZnO nanorods with 5 mM doping concentration; the lowest doping concentration. A sharp increase intensity after threshold was observed in both cases as shown in Fig. 3(b) and (d). However, the threshold power for lasing is at least 10 times smaller in the doped nanorods and the double mode lasing was reduced to single mode, in the case of low pumping energy. For the case of high pumping energy (2 mW in this case), multiple emission modes were still observed as shown in Fig. 2(c); typical for random lasing.

A comparison with other aluminum concentrations as shown in Fig. 4 reveals the same lasing behavior with different values of threshold. The lowest threshold was achieved from ZnO nanorods prepared with 10 mM of aluminum concentration at 5 μW (0.07 W/cm^2) of pump power; almost a factor of 1000 smaller compared to ZnO nanorods without any aluminum impurities. Threshold reduction may be related to the transport mean free path which is affected by changes in rod density, length and size [30]. However, threshold reduction is always less than one order of magnitude [7,11,31,32]. Such large threshold changes, when compared with undoped ZnO, is implying that the aluminum embedded in the nanorods is responsible in reducing the threshold. One possibility is reduced energy transfer to trap state emissions. A similar phenomenon was observed from disordered point-sized structures [33]. When comparing between the doped samples, the difference in threshold reduction is not as large indicating that in this case it is related to the morphology of the sample. As the concentration of aluminum was increased, the threshold increases by a factor of 3 for 30 mM aluminum concentration and by a factor of 50 with 50 mM alumina concentration. Increasing alumina concentration affected the growth of ZnO nanorods and may correspondingly affect the lasing threshold. For the sample

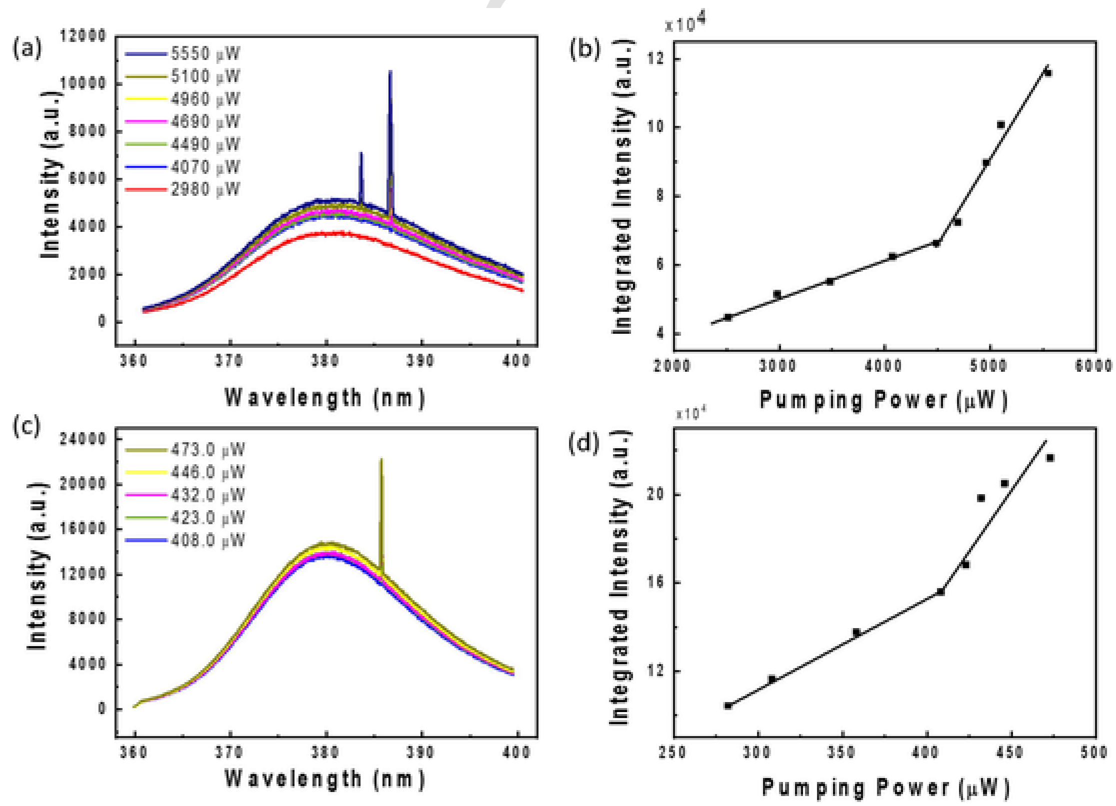

Fig. 3. (a) and (b) Pump power dependence lasing measurement and integrated intensity of the lasing line with pump power from pure ZnO nanorods, (c) and (d) Pump power dependence lasing measurement and integrated intensity of lasing line against pump power from Al-doped ZnO nanorods with 5 mM of Al concentration.

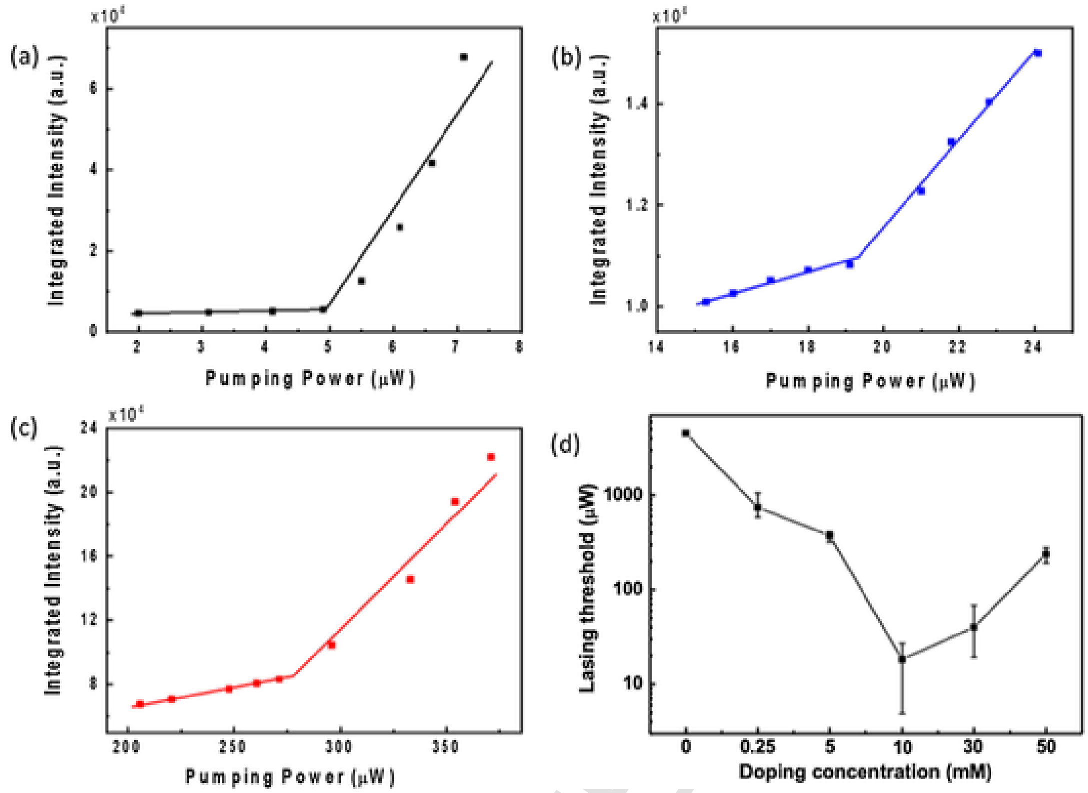

Fig. 4. (a–c) Integrated lasing intensity against pumping power for ZnO naorods with aluminum concentrations of 10 mM, 30 mM and 50 mM respectively. (d) Comparison of lasing threshold for each doping concentration.

with 10 mM alumina concentration, the average density is 153 nanorods/μm^2 and average nanorod diameter is about 34 nm which corresponds to a filling factor of about 0.14. Similar filling factor was reported in another ZnO array system that showed random lasing however, the lowest threshold achieved in our system is 100 times smaller than that reported in [7]. This again confirms the aluminum doping may be responsible in reducing the threshold in ZnO random lasers. When the concentration of alumina increases, the density of nanorods decreases by 30% and threshold increases 3 times as shown in Fig. 3(d).

The emission from ZnO nanorods with 10 mM alumina concentration (lowest threshold) is shown in Fig. 5(a) and a close up of the lasing emission is shown in Fig. 5(b). The lasing mode increases rapidly upon achieving threshold, a typical observation of random lasing. The linewidth was less than 0.4 nm for all the emission peaks upon reaching threshold and is the same for all samples. Conventionally in random lasers the shift can be up to several nm and more modes would appear in the spectrum with increasing pump power. However, upon close up of the lasing emission as shown in Fig. 4(b), shift in lasing wavelength with increasing pump power was less than 0.05 nm and no additional peaks appeared indicating the stability of the lasing emission. Fixed number of modes with increasing pump power has been observed in our previous work from ZnO nanorod matts however there was a shift in wavelength with increasing pump power between 0.2 nm and 0.5 nm depending on the morphology of the sample [11,32,35]. The stability of the lasing emission from this work suggests that slight doping in preparing ZnO nanorods using chemical bath deposition method is a good way of making stable random lasers. Future work may include a comparison with high quality ZnO whereby the green emission is sufficiently suppressed. We believe that our findings spark more experimental

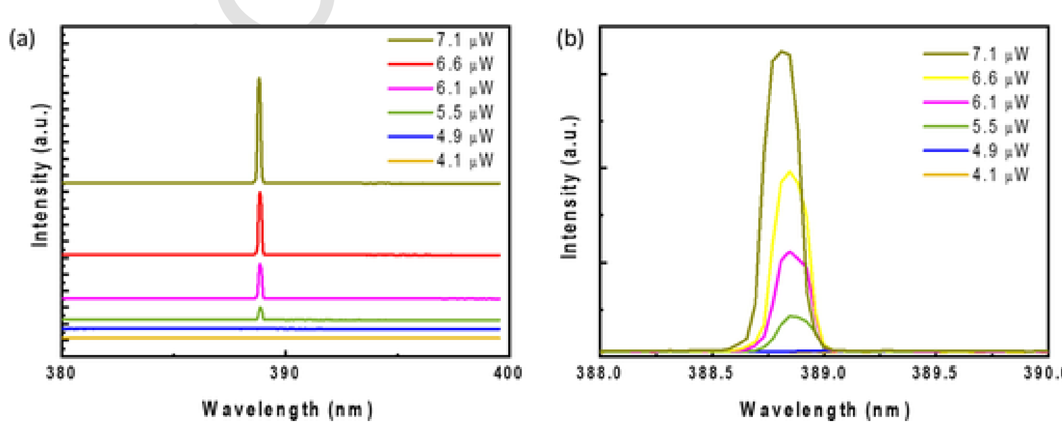

Fig. 5. (a–b) Lasing power dependence measurement and zoomed spectra of the lasing mode from ZnO nanorods doped with 10 mM alumina concentration.

and theoretical works in looking at the effects of doping on random lasing.

4. Conclusion

Random lasing from ZnO nanorods doped with different concentrations of alumina revealed changes in morphology that has reduced the threshold in lasing emission. Threshold was 2 magnitude lower than undoped ZnO possibly due to the aluminum embedded in the ZnO nanorods. Lowest threshold of 5 μW corresponding to just 0.07 W/cm^2 was observed from ZnO nanorods prepared with 10 mM of alumina concentration. Increasing the concentration further increases the threshold. Results suggest doping affects random lasing and opens doors to further investigation in choosing appropriate doping material for a more stable random laser.

Uncited references

.

CRediT authorship contribution statement

N. Fadzliana: Methodology, Formal analysis, Investigation. **S.A.M. Samsuri:** Growth methadology . **S.Y. Chan:** Investigation, Formal analysis. **H.C. Hsu:** Validation, Resources, Writing - review & editing. **W. Maryam:** Conceptualization, Data curation, Validation, Resources, Writing - original draft, Project administration, Funding acquisition.

Declaration of Competing Interest

All authors declare no conflict of interest.

Acknowledgements

The authors are grateful for funding from USM Bridging grant [304/PFIZIK/6316077] and The Ministry of Science and Technology of Taiwan (MOST 105-2112-M-006-004-MY3).

References

[1] X.H. Wu, A. Yamilov, H. Noh, H. Cao, E.W. Seelig, R.P.H. Chang, Random lasing in closely packed resonant scatterers, J. Opt. Soc. Am. B 21 (1) (2004) 159.
[2] L. Zhang, Y. Xu, S. Gao, B. Saxena, L. Chen, X. Bao, Multiwavelength Coherent Brillouin Random Fiber Laser With Ultrahigh Optical Signal-to-Noise Ratio, IEEE J. Sel. Top. Quantum Electron. 24 (3) (May 2018) 1–8.
[3] A. Safdar, Y. Wang, T.F. Krauss, Random lasing in uniform perovskite thin films, Opt. Express 26 (2) (2018) A75.
[4] K. Sarkar, S. Mukherjee, G. Wiederrecht, R.D. Schaller, D.J. Gosztola, M.A. Stroscio, M. Dutta, Ultrafast carrier dynamics and optical pumping of lasing from Ar-plasma treated ZnO nanoribbons, Nanotechnology 29 (9) (2018) 95701, doi:10.1088/1361-6528/aaa530.
[5] S.H. Choi, et al., Anderson light localization in biological nanostructures of native silk, Nat. Commun. 9 (1) (2018) 1–14.
[6] H. Fujiwara, R. Niyuki, K. Sasaki, White light induced photo-thermal switching in a graphene-flake-mixed ZnO nanoparticle random laser, J. Phys. Commun. 2 (3) (Mar. 2018) 035022.
[7] H. Fujiwara, T. Suzuki, R. Niyuki, K. Sasaki, ZnO nanorod array random lasers fabricated by a laser-induced hydrothermal synthesis, New J. Phys. 18 (10) (Oct. 2016) 103046.
[8] H. Fujiwara, R. Niyuki, Y. Ishikawa, N. Koshizaki, T. Tsuji, K. Sasaki, Low-threshold and quasi-single-mode random laser within a submicrometer-sized ZnO spherical particle film, Appl. Phys. Lett. 102 (6) (Feb. 2013) 061110.
[9] H. Zhu, et al., Low-threshold GaN thin-film random laser through the weak scattering feedback, J. Phys. D. Appl. Phys. 50 (4) (Feb. 2017) 045107.
[10] C.-H. Lu, T.-Y. Chao, Y.-F. Chiu, S.-Y. Tseng, H.-C. Hsu, Enhanced optical confinement and lasing characteristics of individual urchin-like ZnO microstructures prepared by oxidation of metallic Zn, Nanoscale Res. Lett. 9 (1) (2014) 178.
[11] W. Maryam, N. Fazrina, M.R. Hashim, H.C. Hsu, M.M. Halim, Optically driven random lasing in ZnO nanorods prepared by chemical bath deposition, Photonics Nanostructures - Fundam. Appl. 26 (Sep. 2017) 52–55.
[12] W.Z.W. Ismail, D. Liu, S. Clement, D.W. Coutts, E.M. Goldys, J.M. Dawes, Spectral and coherence signatures of threshold in random lasers, J. Opt. 16 (10) (Oct. 2014) 105008.
[13] W.Z. Wan Ismail, G. Liu, K. Zhang, E.M. Goldys, J.M. Dawes, Dopamine sensing and measurement using threshold and spectral measurements in random lasers, Opt. Express 24 (2) (2016) A85.
[14] J.A. Copeland, Heavily Doped Semiconductor Lasers, IEEE J. Quantum Electron. 17 (11) (1981) 2187–2190.
[15] T. Schweizer, D.W. Hewak, D.N. Payne, T. Jensen, G. Huber, Rare-earth doped chalcogenide glass laser, Electron. Lett. 32 (7) (1996) 666.
[16] A.V. Marchevsky, J. Mørk, K. Yvind, Doping technologies for InP membranes on silicon for nanolasers, Novel In-Plane Semiconductor Lasers XVIII, 2019, p. 29.
[17] C.-H. Park, M. Yako, K. Wada, Y. Ishikawa, D. Ahn, High concentration phosphorus doping in Ge for CMOS-integrated laser applications, Solid. State. Electron. 154 (Apr. 2019) 43–49.
[18] C.B. Su, V. Lanzisera, Effect of doping level on the gain constant and modulation bandwidth of InGaAsP semiconductor lasers, Appl. Phys. Lett. 45 (12) (Dec. 1984) 1302–1304.
[19] Y. Fujimoto, M. Nakatsuka, Optical amplification in bismuth-doped silica glass, Appl. Phys. Lett. 82 (19) (May 2003) 3325–3326.
[20] N.B. Tomazio, L.F. Sciuti, G.F.B. Almeida, L. De Boni, C.R. Mendonça, Dye-doped random microlasers fabricated via femtosecond laser-induced two-photon polymerization (Conference Presentation), Organic Photonic Materials and Devices XXI, 2019, p. 31.
[21] R. Niyuki, H. Fujiwara, Y. Ishikawa, N. Koshizaki, T. Tsuji, K. Sasaki, Toward single-mode random lasing within a submicrometre-sized spherical ZnO particle film, J. Opt. 18 (3) (Mar. 2016) 035202.
[22] L.L. Yang, Q.X. Zhao, M. Willander, Size-controlled growth of well-aligned ZnO nanorod arrays with two-step chemical bath deposition method, J. Alloys Compd. 469 (1–2) (2009) 623–629.
[23] G. Jia, Y. Wang, J. Yao, Growth mechnism of Zno nano-structure using chemical bath deposition, J. Ovonic Res. 6 (6) (2010) 303–307.
[24] S. Edinger, et al., Comparison of chemical bath-deposited ZnO films doped with Al, Ga and In, J. Mater. Sci. 52 (16) (Aug. 2017) 9410–9423.
[25] P.K. Samanta, A.K. Bandyopadhyay, Chemical growth of hexagonal zinc oxide nanorods and their optical properties, Appl. Nanosci. 2 (2) (Jun. 2012) 111–117.
[26] S.W. Xue, X.T. Zu, W.G. Zheng, M.Y. Chen, X. Xiang, Effects of annealing and dopant concentration on the optical characteristics of ZnO: Al thin films by sol–gel technique, Phys. B Condens. Matter 382 (1–2) (Jun. 2006) 201–204.
[27] A. Mohanta, J.G. Simmons, G. Shen, S.M. Kim, P. Kung, H.O. Everitt, Al doping in ZnO nanowires enhances ultraviolet emission and suppresses broad defect emission, J. Lumin. 211 (Jul. 2019) 264–270.
[28] D. Thomas, K.K. Sadasivuni, S. Waseem, B. Kumar, J.-J. Cabibihan, Synthesis, green emission and photosensitivity of Al-doped ZnO film, Microsyst. Technol. 24 (7) (Jul. 2018) 3069–3073.
[29] Y. Geng, et al., Influence of Al Doping on the Properties of ZnO Thin Films Grown by Atomic Layer Deposition, J. Phys. Chem. C 115 (25) (Jun. 2011) 12317–12321.
[30] P.D. García, C. López, From Bloch to random lasing in ZnO self-assembled nanostructures, J. Mater. Chem. C 1 (44) (2013) 7357–7362.
[31] H. Cao, Y. Zhao, S. Ho, E. Seelig, Q. Wang, R. Chang, Random laser action in semiconductor powder, Phys. Rev. Lett. 82 (11) (Mar. 1999) 2278–2281.
[32] W.M. Wan Ahmad Kamil, M.K. Shakfa, M.N. Nordin, D. Priante, Lasing from ZnO nanorods prepared on ITO-coated substrate, in: Semiconductor Lasers and Laser Dynamics VIII, 2018, no. May, p. 27.
[33] R. Bardoux et al., Single mode emission and non-stochastic laser system based on disordered point-sized structures : toward a tuneable random laser, 19(10) (2011), pp. 9262–9268.
[35] N.I.M. Tazri, O.L. Muskens, M.K. Shakfa, W. Maryam, Polycrystalline ZnO nanorods for lasing applications, J. Appl. Phys. 125 (12) (Mar. 2019) 123103.
[36] X.H. Wu, A. Yamilov, H. Noh, H. Cao, E.W. Seelig, R.P.H. Chang, Journal of the Optical Society of America B 21 (2004), doi:10.1364/JOSAB.21.000159.